Search for Cosmic-Ray Antideuterons with BESS-Polar II

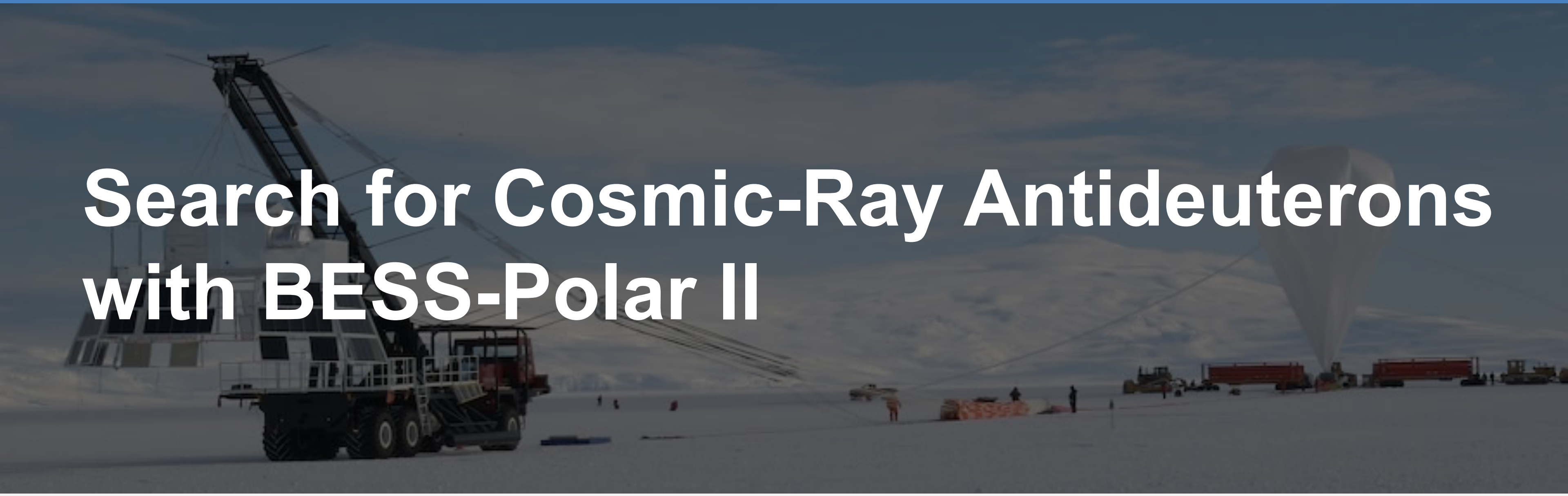

Kenichi Sakai
NASA/GSFC/CRESST/UMBC

For BESS collaboration

Antideuteron 2019
University of California Los Angeles
27-29 March 2019

d19

1 BESS collaboration

BESS is US-Japan collaborative program.

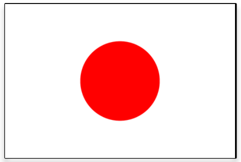

J. W. Mitchell (PI, US, NASA/GSFC)

A. Yamamoto (PI, Japan, KEK)

National Aeronautical and Space Administration / Goddard Space Flight Center (NASA/GSFC)

University of Maryland

University of Denver
(Since June 2005)

High Energy Accelerator Research Organization (KEK)

The University of Tokyo

Kobe University

Institute of Space and Astronautical Science/JAXA

2 BESS-Polar I and II experiment

BESS-Polar I & II flights were carried out over Antarctica.

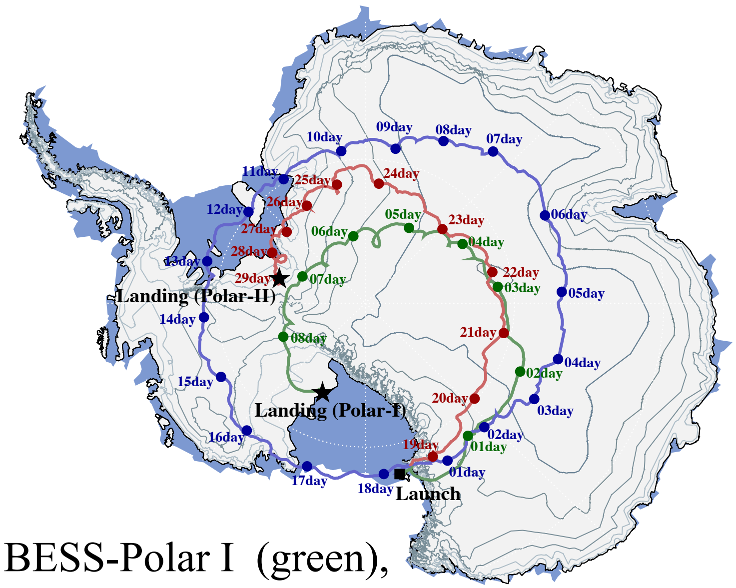

BESS-Polar I (green),
BESS-Polar II (1^{st} :blue, 2^{nd} :red)

	BESS-Polar I	BESS-Polar II
Launch date	Dec. 13th ,2004	Dec. 23rd , 2007
Observation time	8.5 days	24.5 days
Cosmic-ray observed	9 x 10^8 events	4.7 x 10^9 events
Flight altitude	37~39km (5~4g/cm^2)	~36km (6~5g/cm^2)

3 BESS spectrometer

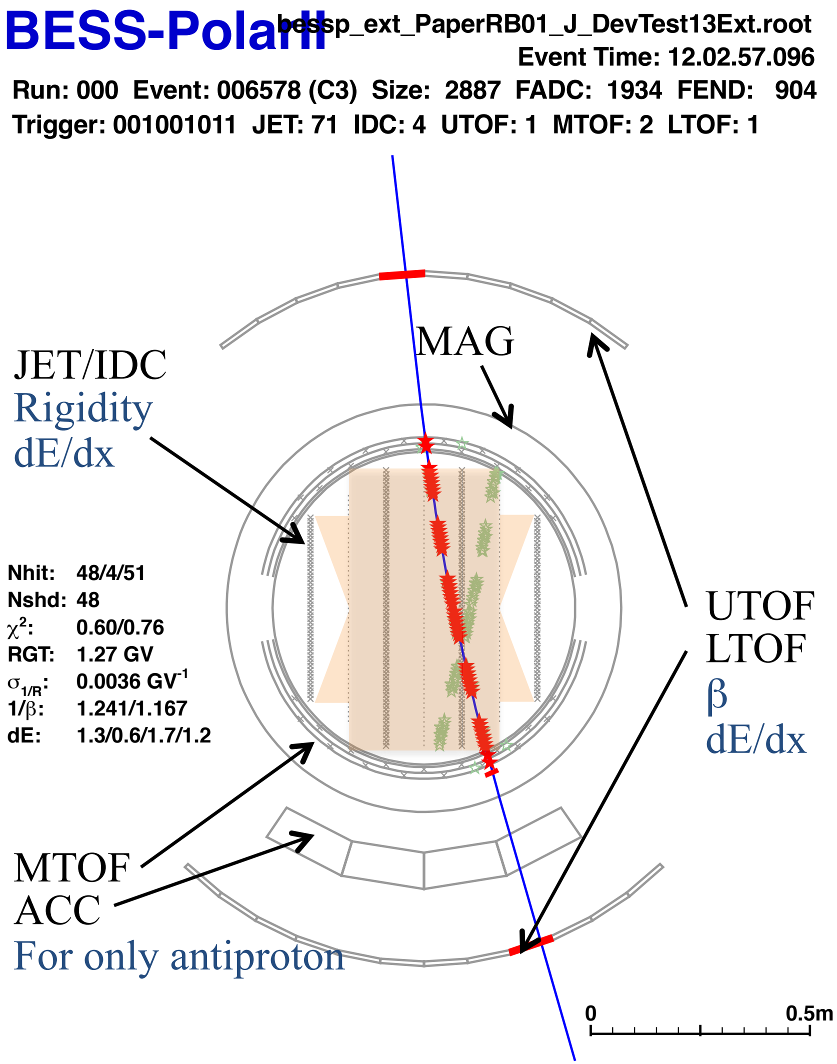

Event display with reconstructed proton track is shown.

Rigidity (MDR:200GV)

Solenoid: Uniform field (ϕ=0.9m, B=0.8T)
Thin material (2.4 g/cm^2/wall)

Drift chamber: Redundant hits
(σ~150μm, 32~48+4hits)

Charge, Velocity

TOF, Chamber: dE/dx measurement
(Z = 1, 2, ...)

TOF: 1/β measurement (σ~1,2%)

$$m = ZeR\sqrt{1/\beta^2 - 1}$$

4 Antiparticle Results from BESS

Antiproton	Antihelium	Antideuteron
BESS-Polar II PRL 108, 051102 (2012)	BESS-Polar II PRL 108, 131301 (2012)	BESS 97-00 PRL 95, 081101 (2005)

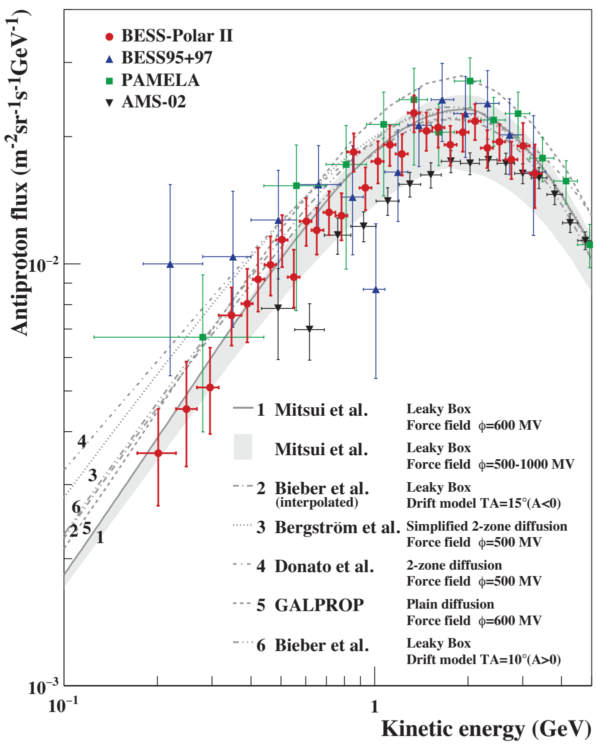

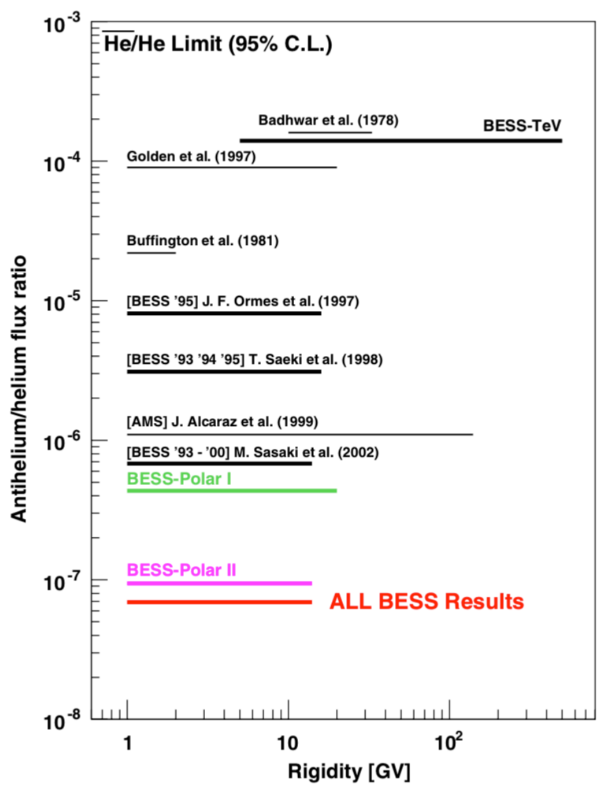

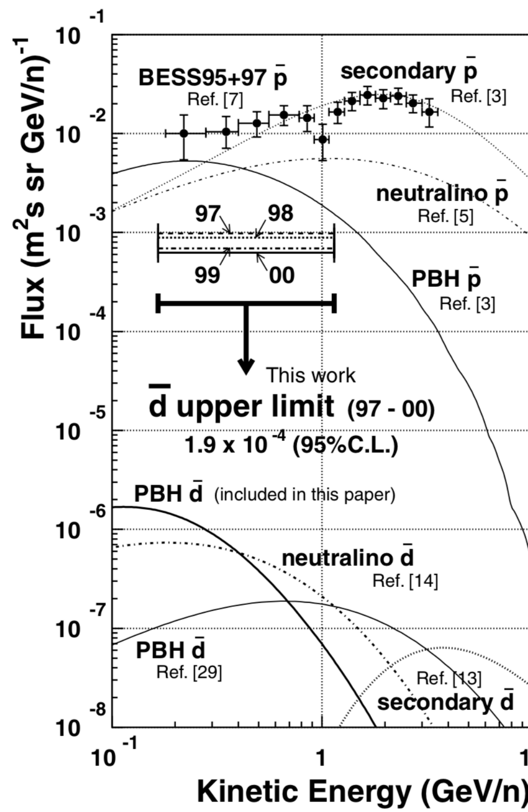

New results of very-low energy Antiproton spectrum by using Middle TOF

Search for Antideuteron **This work** in BESS-Polar II data

Very-low energy antiproton spectrum

5 Minimizing Material in particle path

To minimize material in spectrometer: New detector (Middle TOF)

BESS-2000

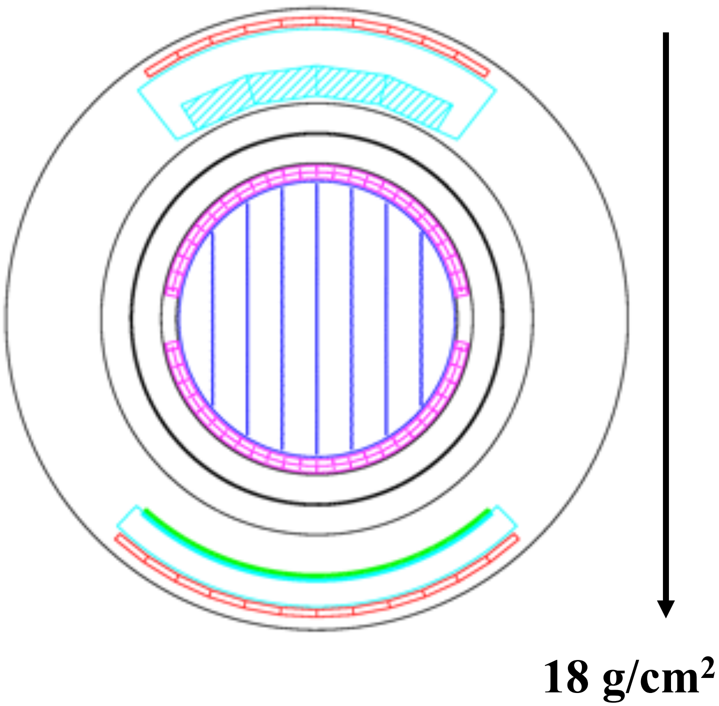

BESS-Polar

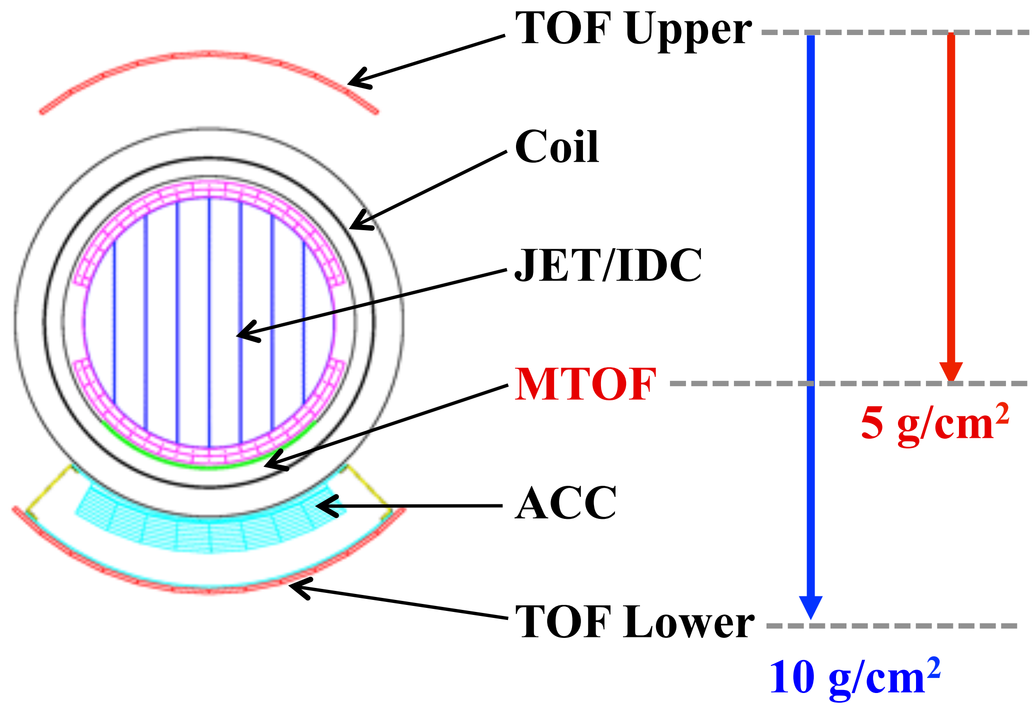

MTOF extends the energy range down to about 0.1 GeV.

6 Antiproton identification

The $1/\beta_{UM}$ VS rigidity plot

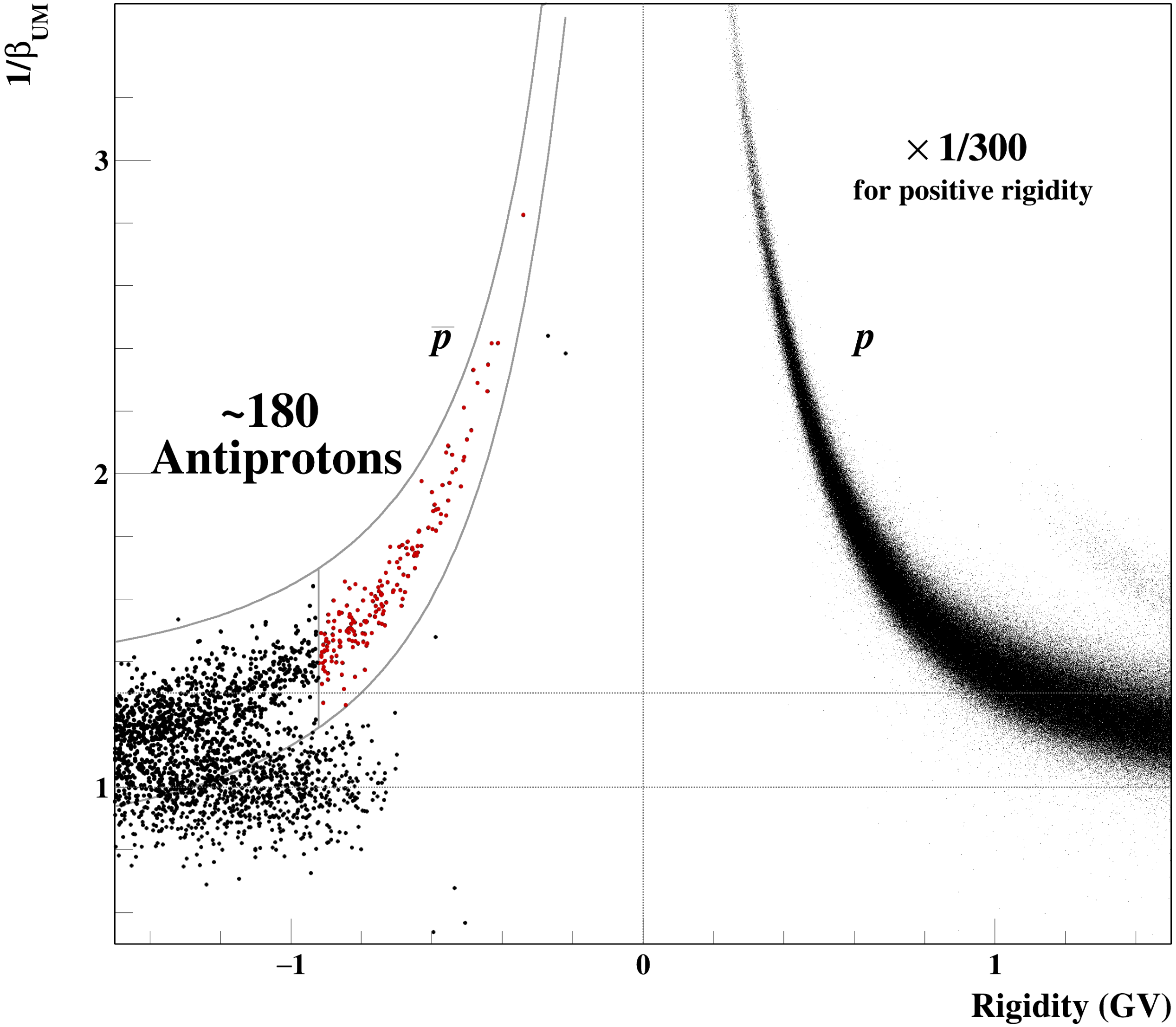

Ref: $1/\beta_{UL}$ VS rigidity

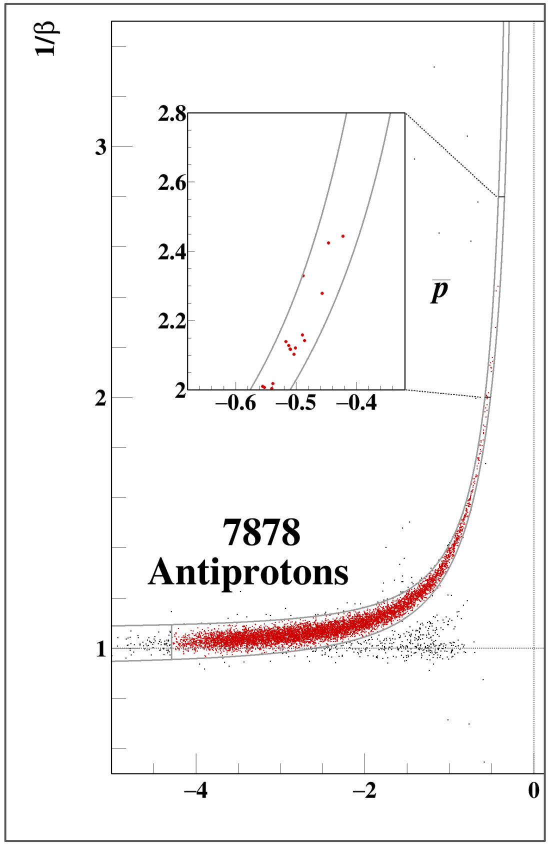

7 Antiproton flux with UTOF-MTOF trigger events

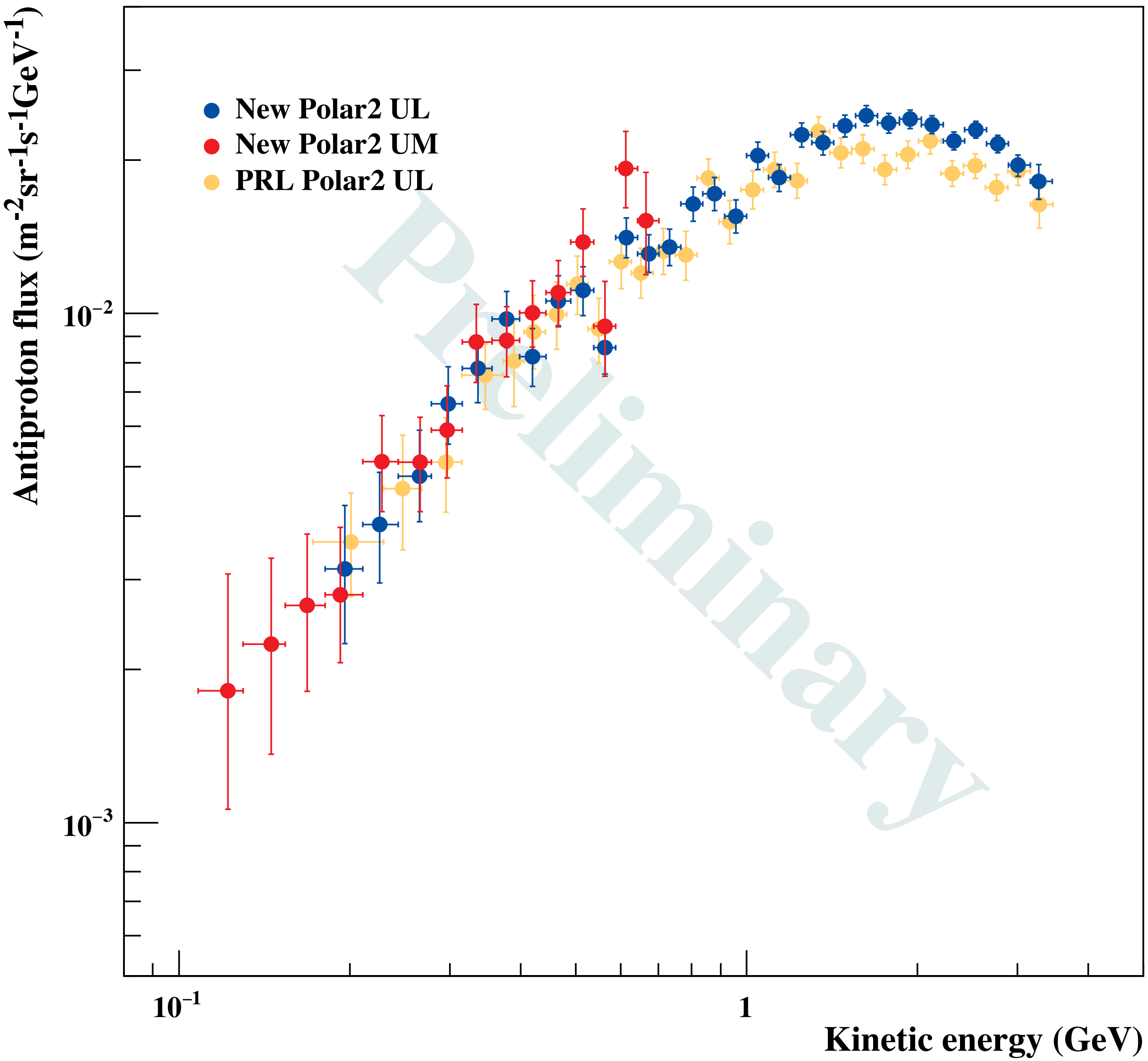

New UM and UL absolute differential energy spectra of antiprotons measured by BESS-Polar II together with earlier published BESS-Polar II UL antiproton spectrum

- UL antiproton flux: 0.2-3.5 GeV
- UM antiproton flux: 0.1-0.7 GeV

8 New antiproton flux in BESS-Polar II

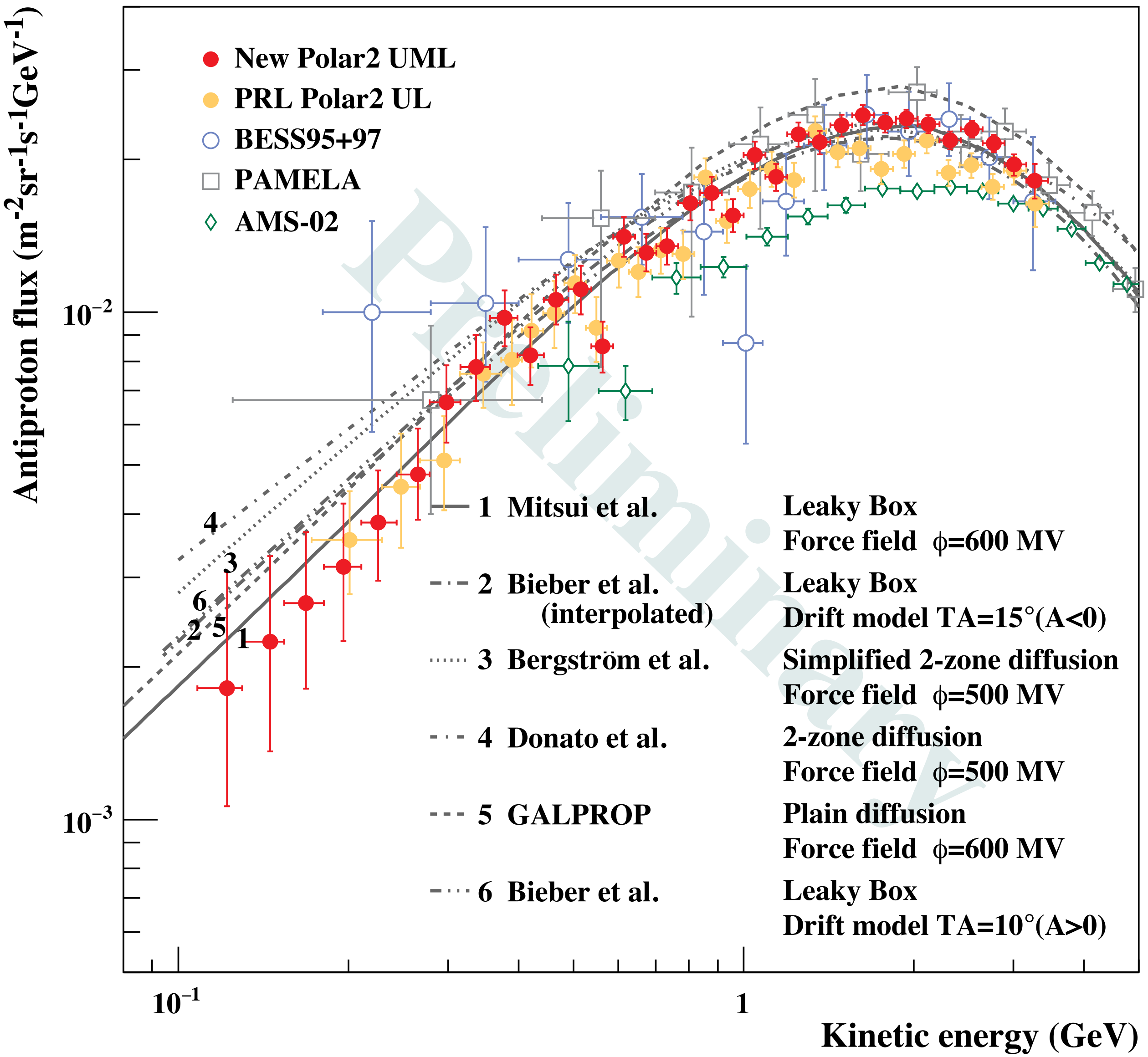

New absolute differential energy spectra of antiprotons measured by BESS-Polar II together with earlier published BESS-Polar II UL antiproton spectrum

- New antiproton flux shows good consistency with secondary antiproton spectra.

Antideuteron search

9 Selection criteria of Dbar analysis (Pre-Selection and Fiducial)

Pbar

Pre-selection	UL
Number of long track	$N_{longTK} = 1$
Noise event veto	$N_{SEG} \leqq 20$
Hits in TOF	$N_{TOFU,L} = 1$
Albedo rejection	$\beta > 0$
Rigidity	$Rgt \neq 0$
χ^2 in trajectory fitting	$\chi_{r\phi}^2 > 0$

Fiducial-selection	UL
Expect hits in JET	$N_{expect} \geqq 32$, $N_{center} > 0$
X hit position in TOF	$\lvert X_{TRU,L} \rvert \leqq 50mm$
Z hit position in TOF	$\lvert Z_{TKU,L} \rvert < 450mm$
TOF mask	or: 7, 15
Swivel cut	

Dbar

Pre-selection	UL
Number of long track	$N_{longTK} = 1$
Noise event veto	$N_{SEG} \leqq 20$
Hits in TOF	$N_{TOFU,L} = 1$
Albedo rejection	$\beta > 0$
Rigidity	$Rgt \neq 0$
χ^2 in trajectory fitting	$\chi_{r\phi}^2 > 0$
Reject noisy IDC hits	$N_{IDCU,L} \geqq 3$

Fiducial-selection	UL
Expect hits in JET	$N_{expect} \geqq 32$, $N_{center} \geqq N_{expect} \times 0.65$
X hit position in TOF	$\lvert X_{TRU,L} \rvert \leqq 50mm$
Z hit position in TOF	$\lvert Z_{TKU,L} \rvert < 450mm$
TOF mask	or: 7, 15
Swivel cut	

10 Selection criteria of Dbar analysis (Quality cut)

Pbar

Quality cut	UL
[1] Charge selection	dE/dx_{UTOF} = pbar (A.4)
[2] Charge selection	dE/dx_{LTOF} = pbar (A.4)
[3] Mass selection	$1/\beta$ = pbar (A.4)
[4] Z reconstruction	$\chi_z^2 > 0$, $\chi_z^2 \leqq 4$ $N_{Vernier} \geqq 4$
[5] QDC hazard	
[6] Z track consistency	$dZ_{UTOF} > 0$, $dZ_{LTOF} > 0$ $dZ_{UTOF} \leqq 50$ $dZ_{LTOF} \leqq 50$
[7] rϕ track quality	$C_{r\phi}^2 \leqq 3$ $L_{path} \geqq 500$ N_{JET}/N_{expect} >= 0.6 N_{drop}/N_{expect} <= 0.25 $\Delta_{RT} \leqq 0.015$

Agel cut	UL
Agel Fiducial	acx > -330, acx < 330 acz > -385, acz < 410
Gap cut	acz ~ -128, 147
Threshold	$\Sigma_{agel} \leqq 340$ $\Sigma_{agel} \leqq 1000$ ($1/\beta$>1.2, |Rgt| < 1.8)

Dbar

Quality cut	UL
[1] Charge selection	dE/dx_{UTOF} = dbar (A.4)
[2] Charge selection	dE/dx_{LTOF} = dbar (A.4)
[3] Mass selection	$1/\beta$ = dbar (A.4)
[4] Z reconstruction	$\chi_z^2 > 0$, $\chi_z^2 \leqq 4$ $N_{Vernier} \geqq 4$
[5] QDC hazard	
[6] Z track consistency	$dZ_{UTOF} > 0$, $dZ_{LTOF} > 0$ $dZ_{UTOF} \leqq 50$ $dZ_{LTOF} \leqq 50$
[7] rϕ track quality	$C_{r\phi}^2 \leqq 3$ $L_{path} \geqq 500$ N_{JET}/N_{expect} >= 0.75 N_{drop}/N_{expect} <= 0.25 $\Delta_{RT} \leqq 0.015$

Agel cut	UL
Agel Fiducial	acx > -330, acx < 330 acz > -385, acz < 410
Gap cut	acz ~ -128, 147
Threshold	$\Sigma_{agel} \leqq 100$

11 Other normalization factor and efficiencies

Pbar

Normalization factor	
trigger efficiency	0.9987*0.9987
track-reconstruction efficiency	0.987
probability of events without accidental tracks	0.9630
probability of events without accidental TOF hits	0.997*0.996
Livetime	1.2720e+06

Dbar

Normalization factor	
trigger efficiency	0.9987*0.9987
track-reconstruction efficiency	0.987
probability of events without accidental tracks	0.9630
probability of events without accidental TOF hits	0.997*0.996
Livetime	1.2720e+06

- In general, selection criteria of Dbar analysis are identical to that of Pbar analysis.
- More strict cut of JET/IDC chamber was employed for selecting the good tracking since dbar analysis is a detection study.
- Particle identification with mass and dE/dx band cut was optimized by using deuteron sample instead of proton sample.
- Higher ACC threshold was employed to prevent background contamination.

12 Particle identification

dE/dx

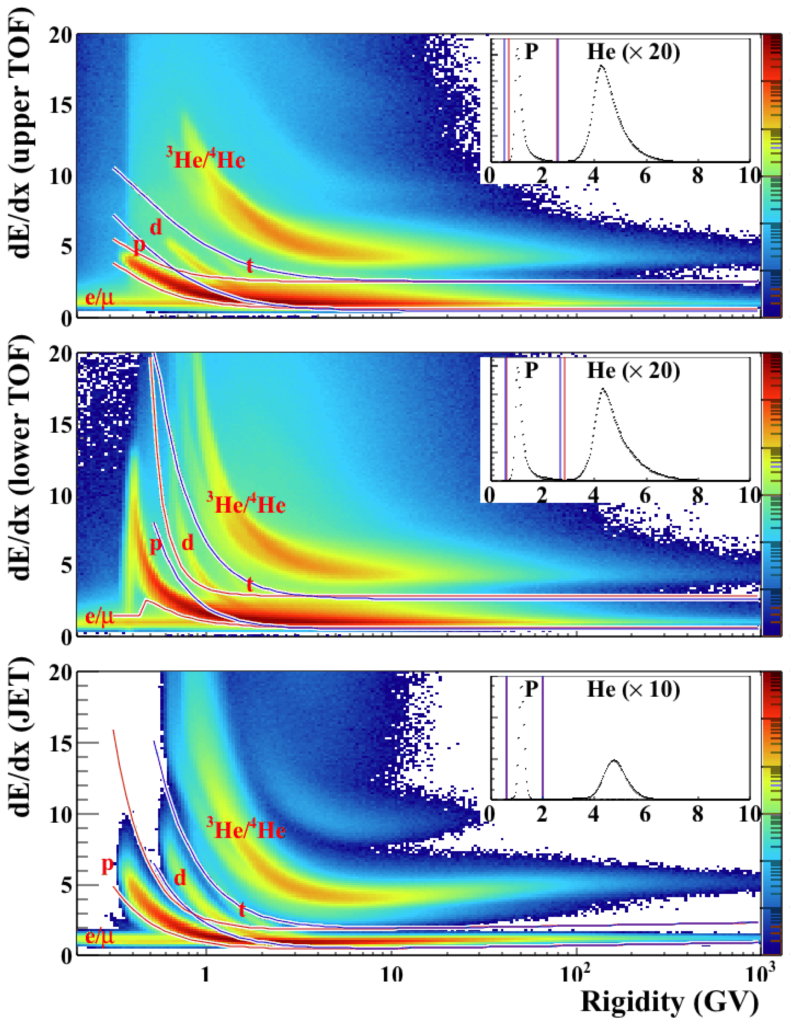

1/β

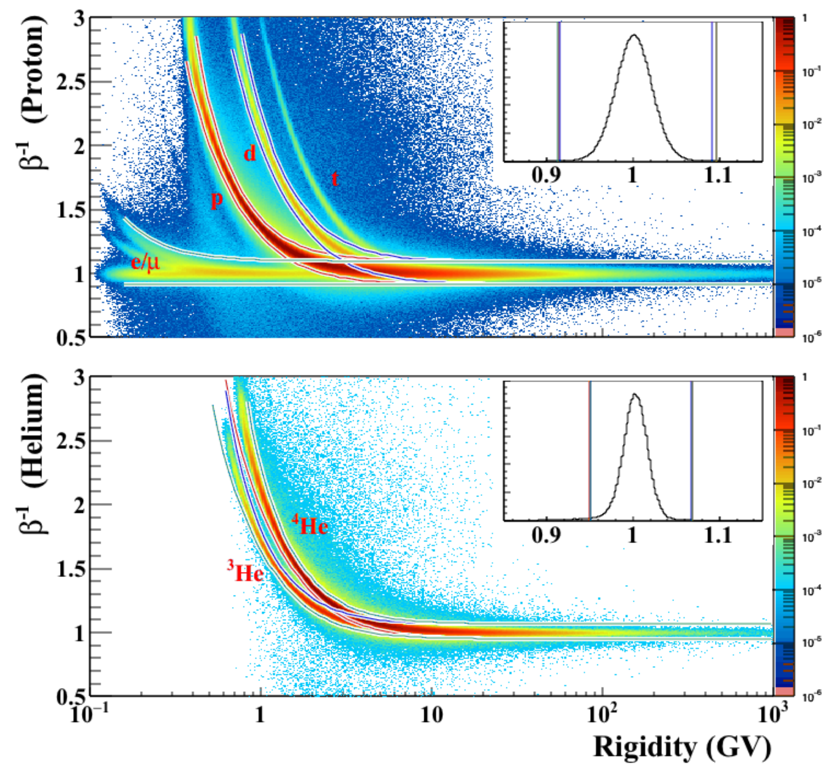

13 ACC rejection power

Pbar (Threshold=340)

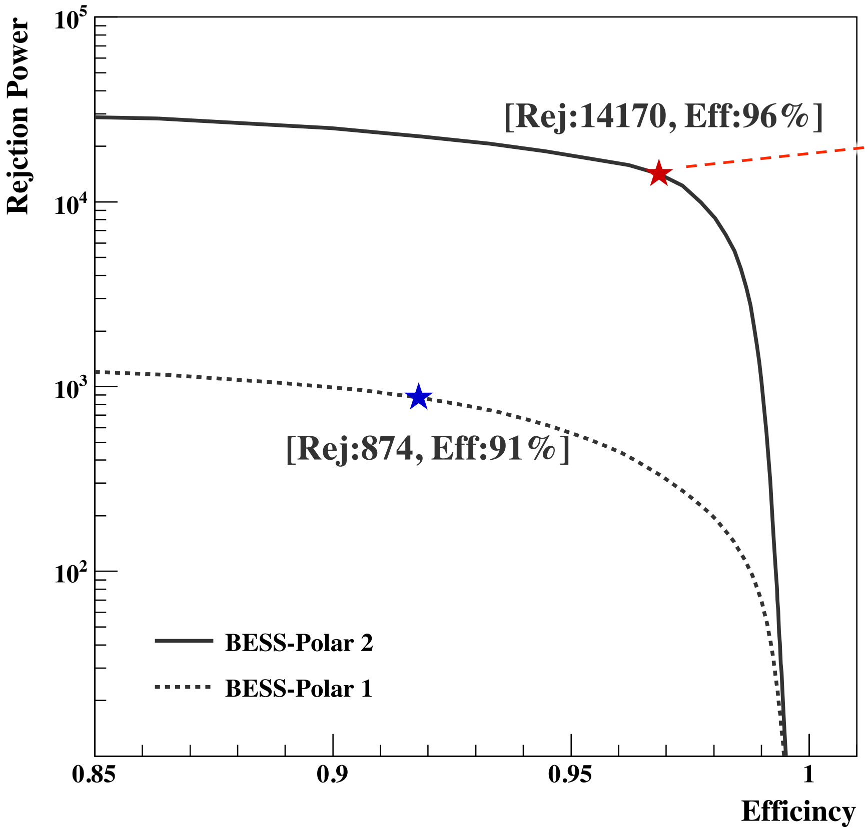

Dbar (Threshold=100)

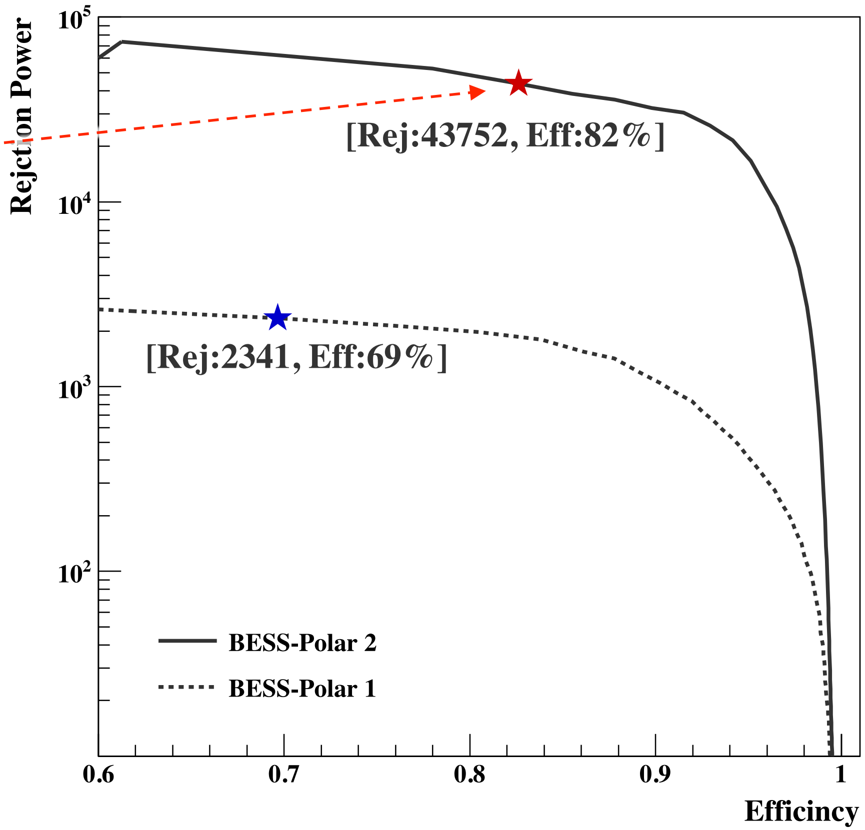

14 Antideuteron search

The $1/\beta_{UL}$ VS rigidity plot

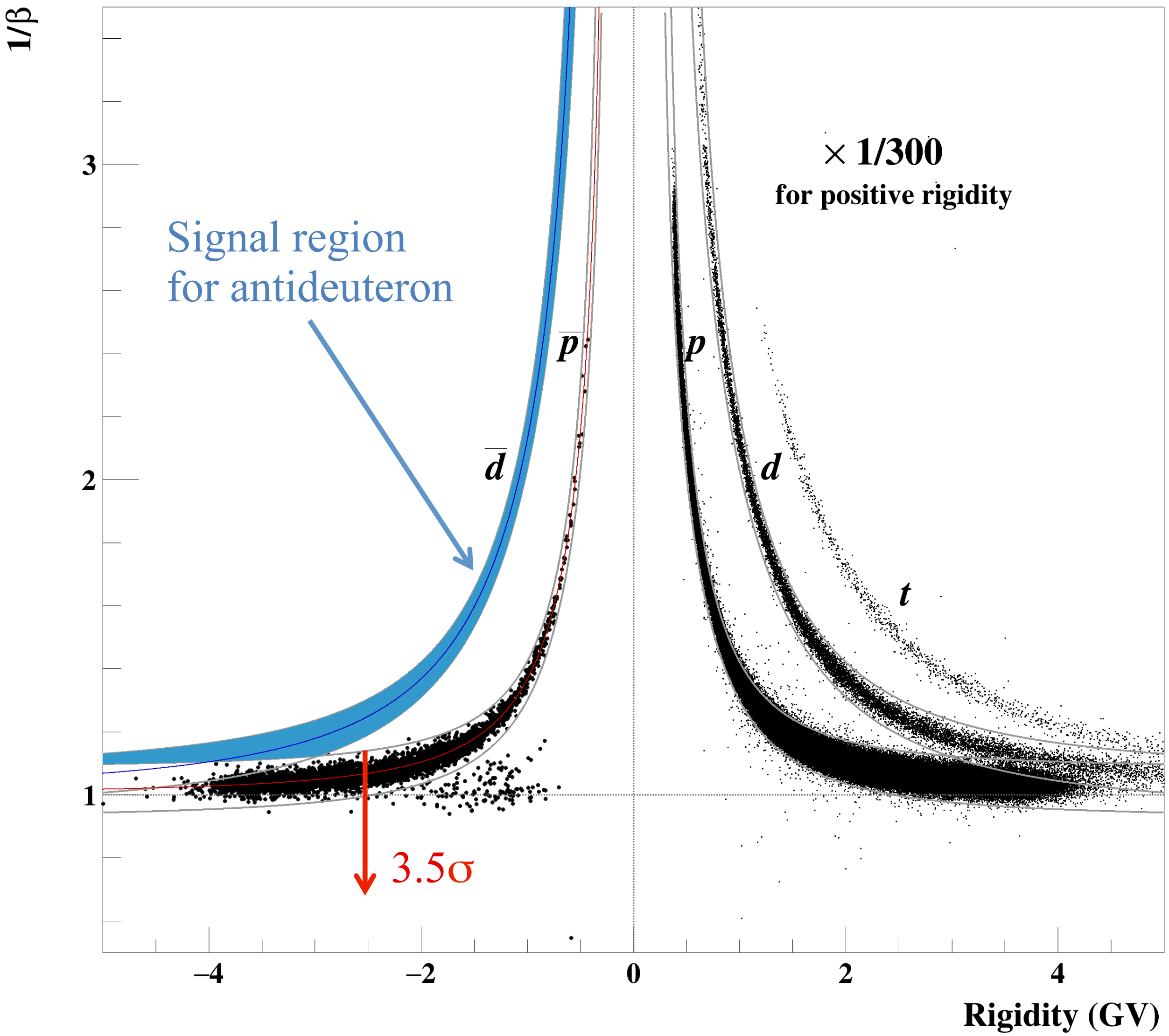

The $1/\beta_{UL}$ VS rigidity plot and antideuteron's selection band.

- Signal region for antideuteron

Excluding 3.5σ region from antiproton center to prevent antiproton contamination

15 Antideuteron search

The $1/\beta_{UL}$ VS rigidity plot

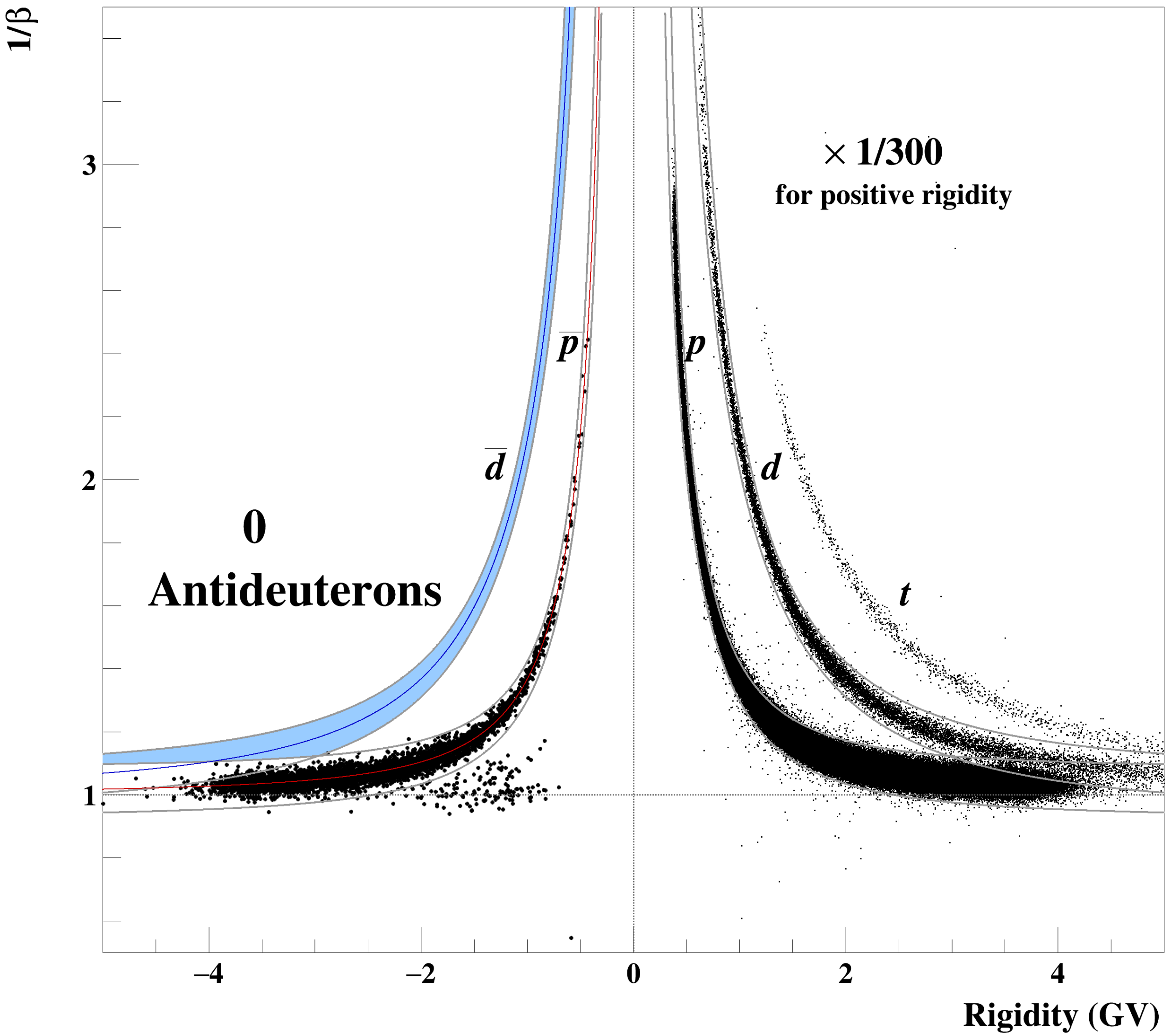

The $1/\beta_{UL}$ VS rigidity plot and antideuteron's selection band.

- Signal region for antideuteron

  Excluding 3.5σ region from antiproton center to prevent antiproton contamination

- No antideuteron candidate in BESS-Polar II data

16 Upper limit calculation

$$\Phi_{\bar{d}}\, dE = \frac{N_{obs}}{S\Omega \cdot T_{live}} \frac{1}{\varepsilon_{single} \cdot \varepsilon_{Q-ID}} \frac{1}{\eta} \frac{1}{(1-\delta_{sys})}$$

N_{obs} : Number of Observed candidate = 3.1
$S\Omega$: Geometrical acceptance
T_{live} : Live time
ε_{single} : Single track efficiency
ε_{Q-ID} : Detector selection efficiencies
η : Survival fraction through atmosphere
δ_{sys} : Systematic error

- Since no antideuteron was found, 3.1 was taken as the number of the observed antideuteron events for the calculation of 95% C.L. upper limit.
- In order to obtain the most conservative limit, the minimum value of the effective exposure factors ($S\Omega \cdot T_{live} \cdot \varepsilon_{single} \cdot \varepsilon_{Q-ID} \cdot \eta$) was used.

17 Extended Agel efficiency by using proton

$$\Phi_{\bar{d}}\, dE = \frac{N_{obs}}{S\Omega \cdot T_{live}} \frac{1}{\varepsilon_{single} \cdot \varepsilon_{Q-ID}} \frac{1}{\eta} \frac{1}{(1-\delta_{sys})}$$

1/β VS rgt

Agel efficiency

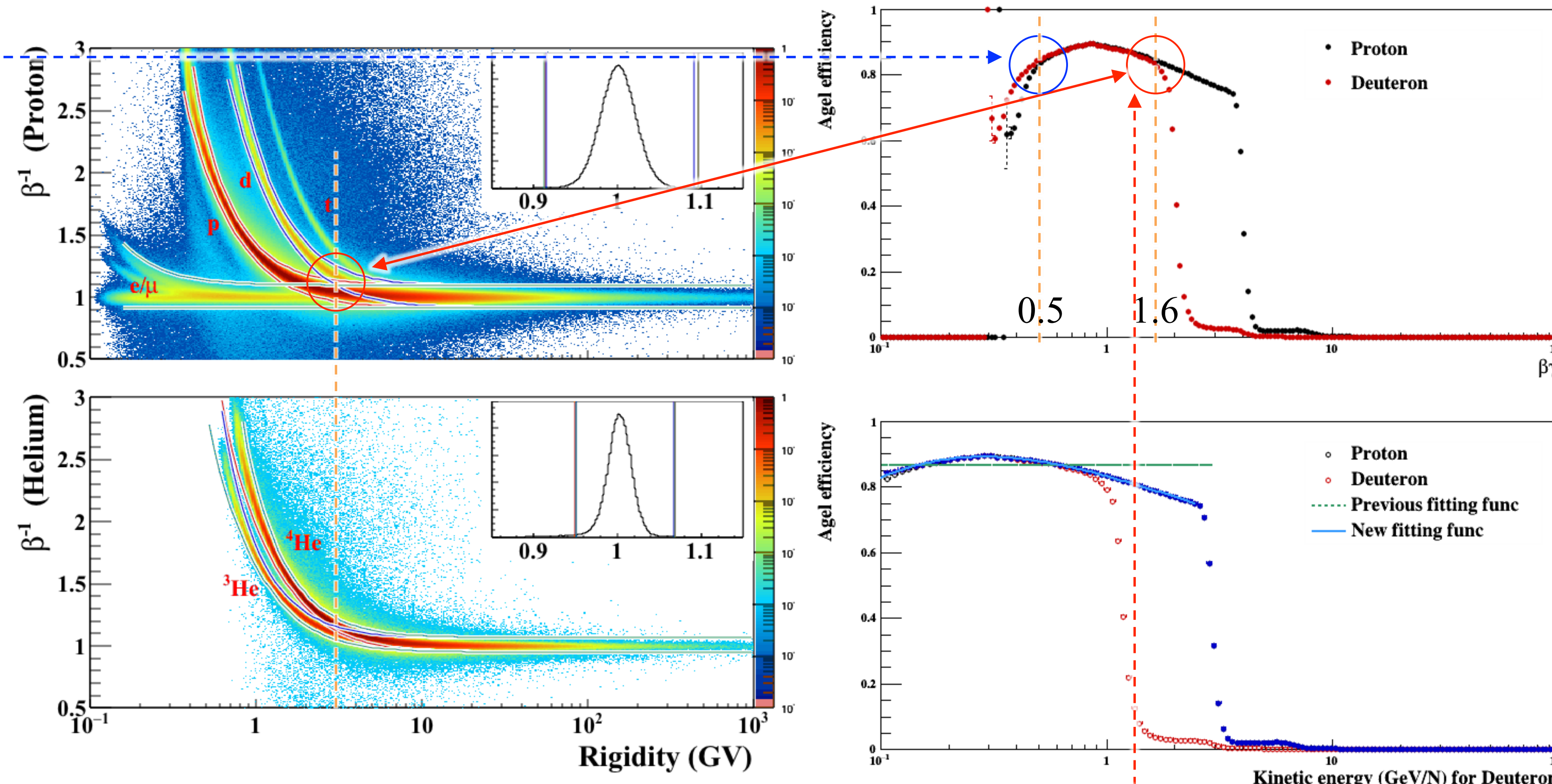

- Due to proton contamination, deuteron aerogel efficiency is miscalculated. Rgt = 3.0GV ⇄ βγ = 1.6 (deuteron), 3.2 (proton)
- Proton efficiency is miscalculated around lower limit of 0.11GeV ⇄ βγ = 0.5.

18 Detector efficiencies

$$\Phi_{\bar{d}}\, dE = \frac{N_{obs}}{S\Omega \cdot T_{live}} \frac{1}{\varepsilon_{single} \cdot \varepsilon_{Q-ID}} \frac{1}{\eta} \frac{1}{(1-\delta_{sys})}$$

Pbar

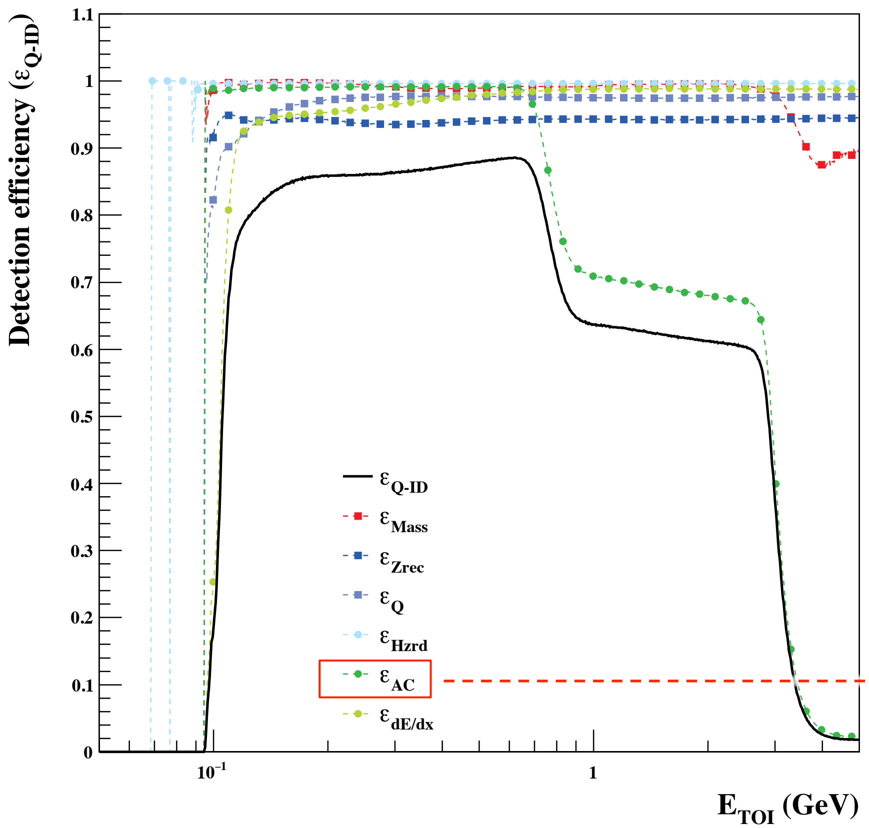

Dbar

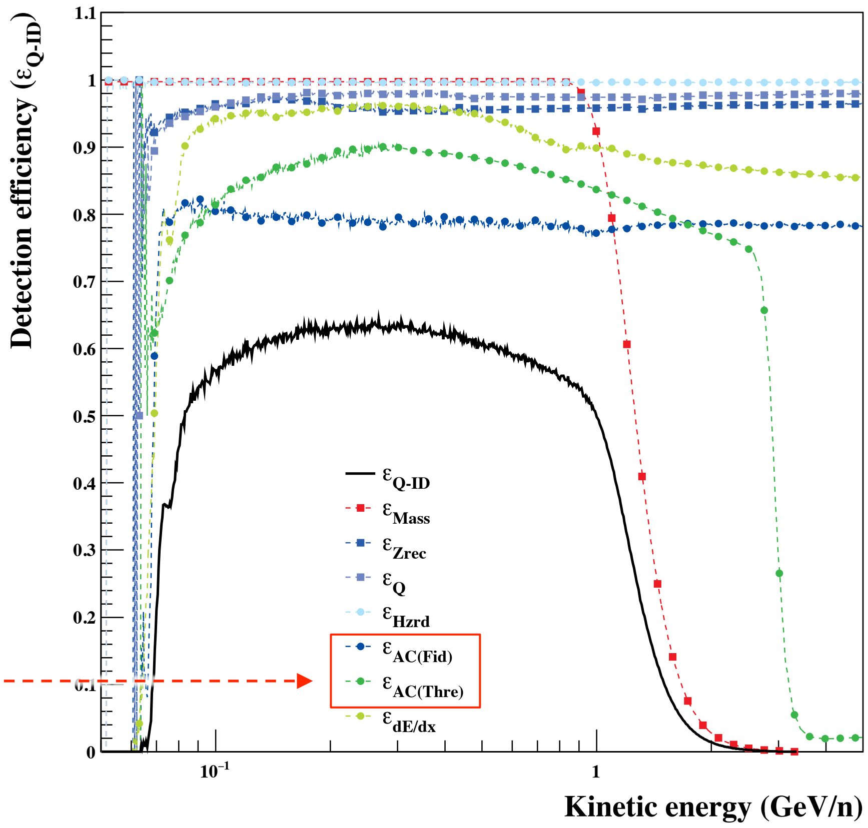

19 Geometrical acceptance x ε_{single}

$$\Phi_{\bar{d}}\, dE = \frac{N_{obs}}{S\Omega \cdot T_{live}} \frac{1}{\varepsilon_{single} \cdot \varepsilon_{Q-ID}} \frac{1}{\eta} \frac{1}{(1-\delta_{sys})}$$

Pbar

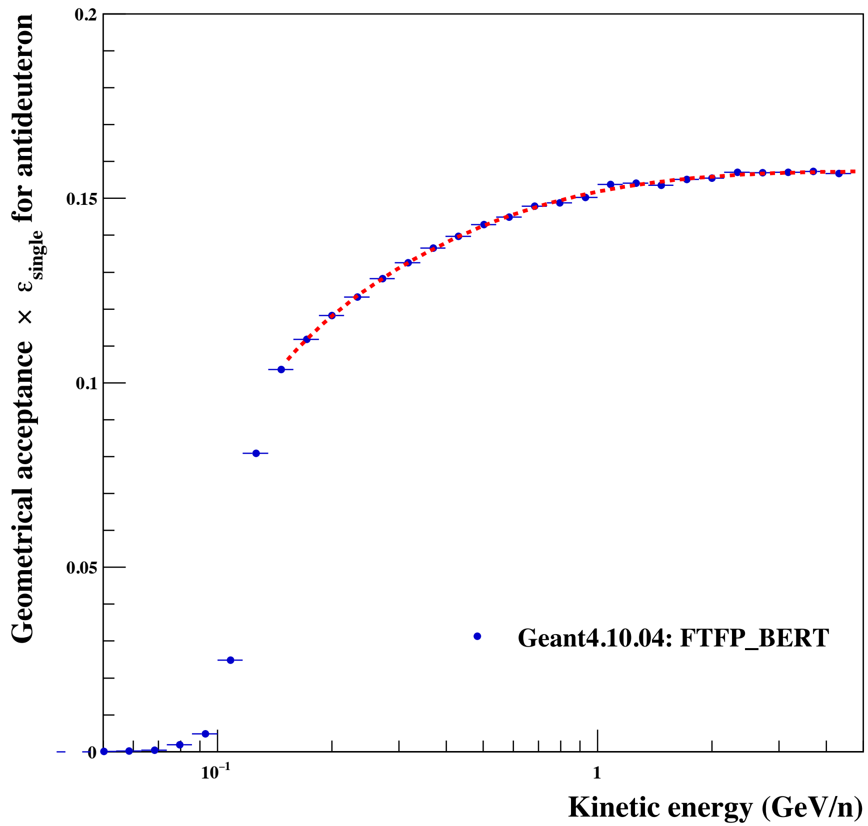

Dbar

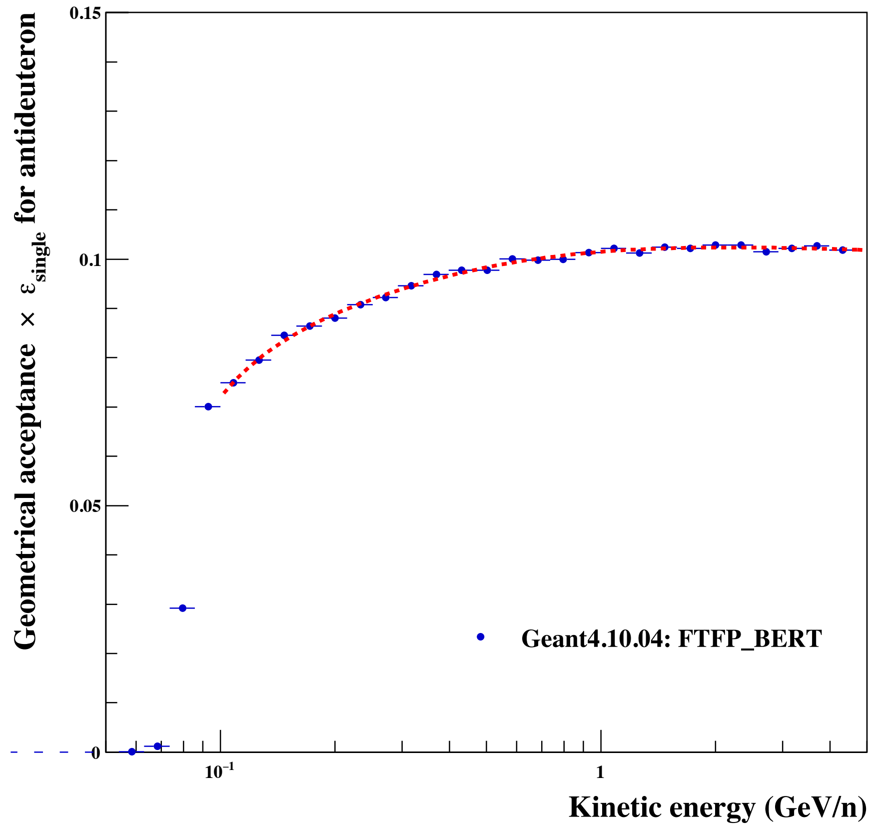

20 Survival prob in the residual atmosphere

$$\Phi_{\bar{d}}\, dE = \frac{N_{obs}}{S\Omega \cdot T_{live}} \frac{1}{\varepsilon_{single} \cdot \varepsilon_{Q-ID}} \frac{1}{\eta} \frac{1}{(1-\delta_{sys})}$$

Pbar

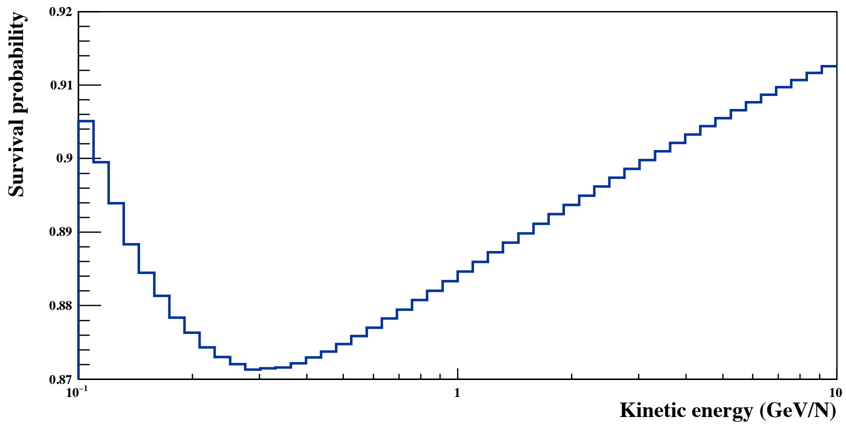

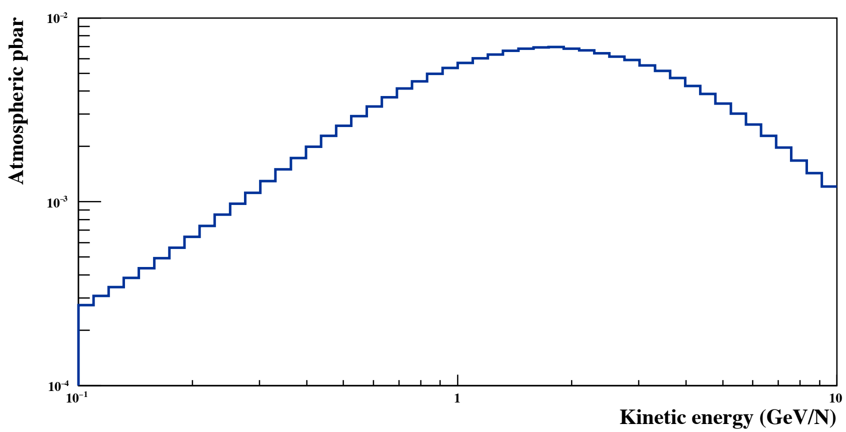

Dbar

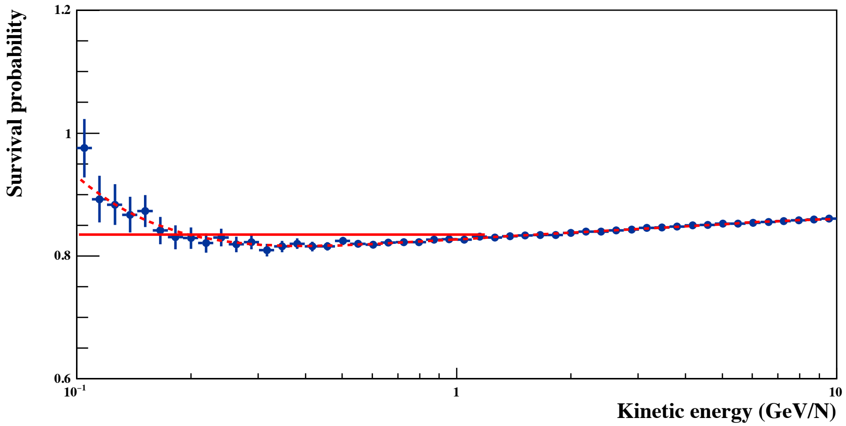

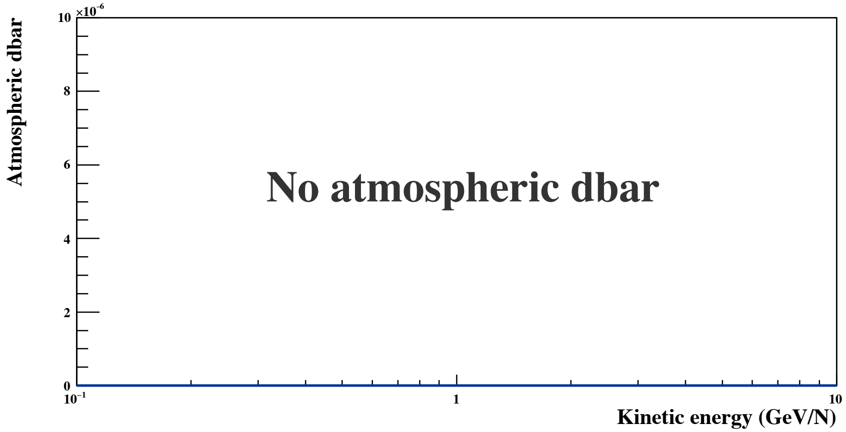

21 Background

$$\Phi_{\bar{d}}\, dE = \frac{N_{obs}}{S\Omega \cdot T_{live}} \frac{1}{\varepsilon_{single} \cdot \varepsilon_{Q-ID}} \frac{1}{\eta} \frac{1}{(1-\delta_{sys})}$$

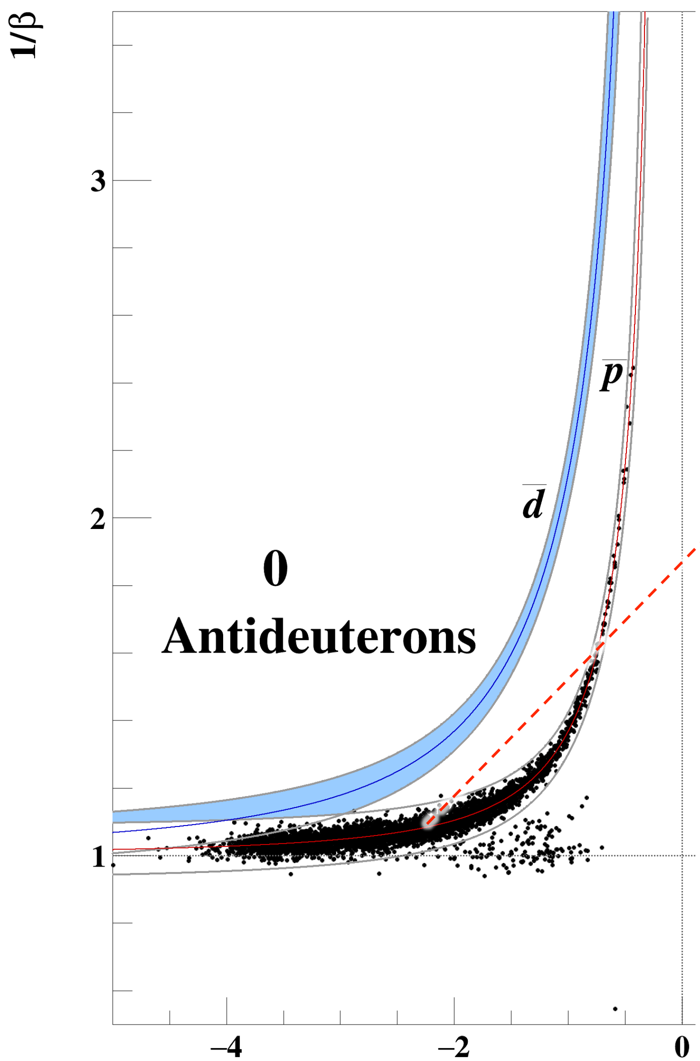

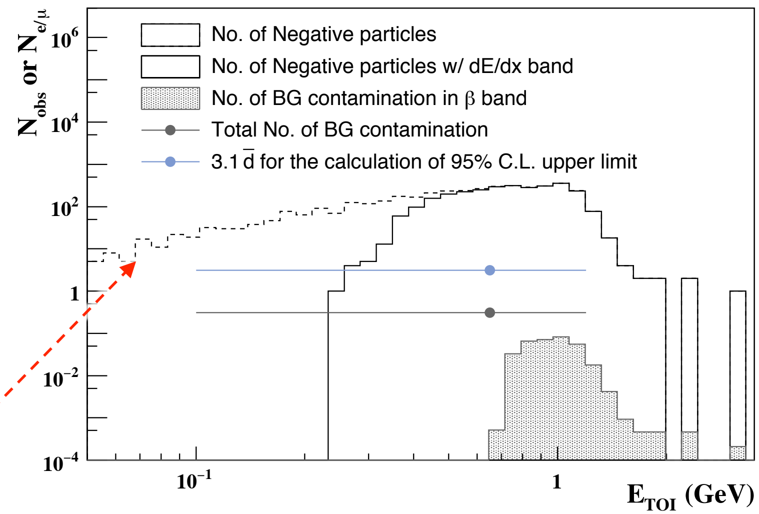

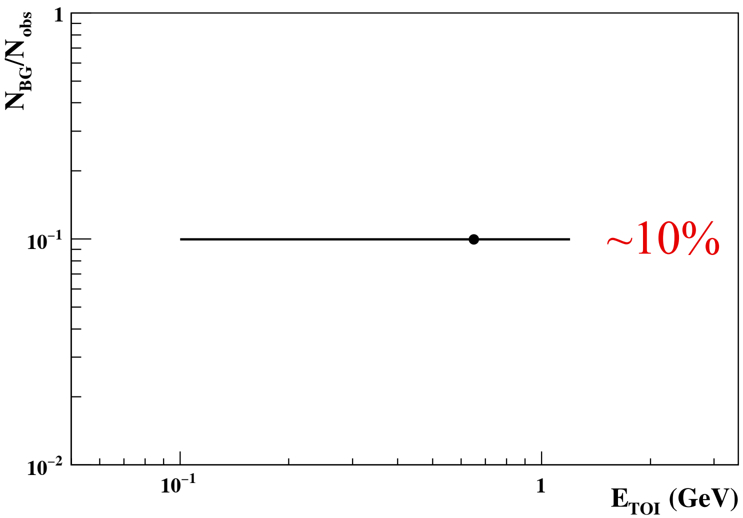

22 Systematic error

$$\Phi_{\bar{d}}\, dE = \frac{N_{obs}}{S\Omega \cdot T_{live}} \frac{1}{\varepsilon_{single} \cdot \varepsilon_{Q-ID}} \frac{1}{\eta} \frac{1}{(1-\delta_{sys})}$$

Pbar

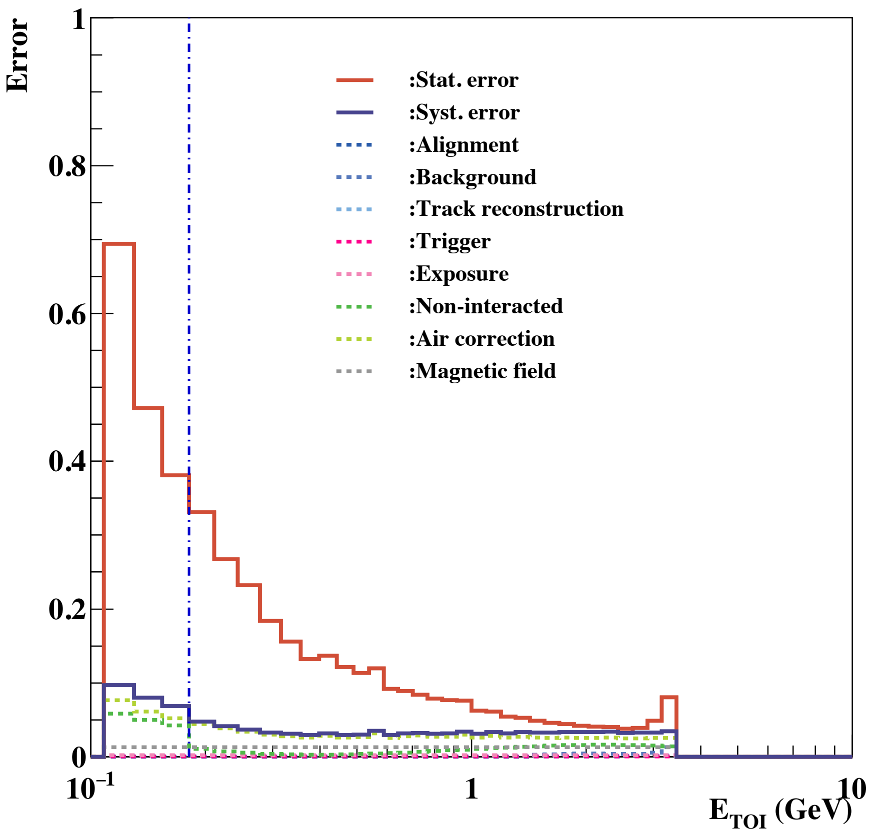

Dbar

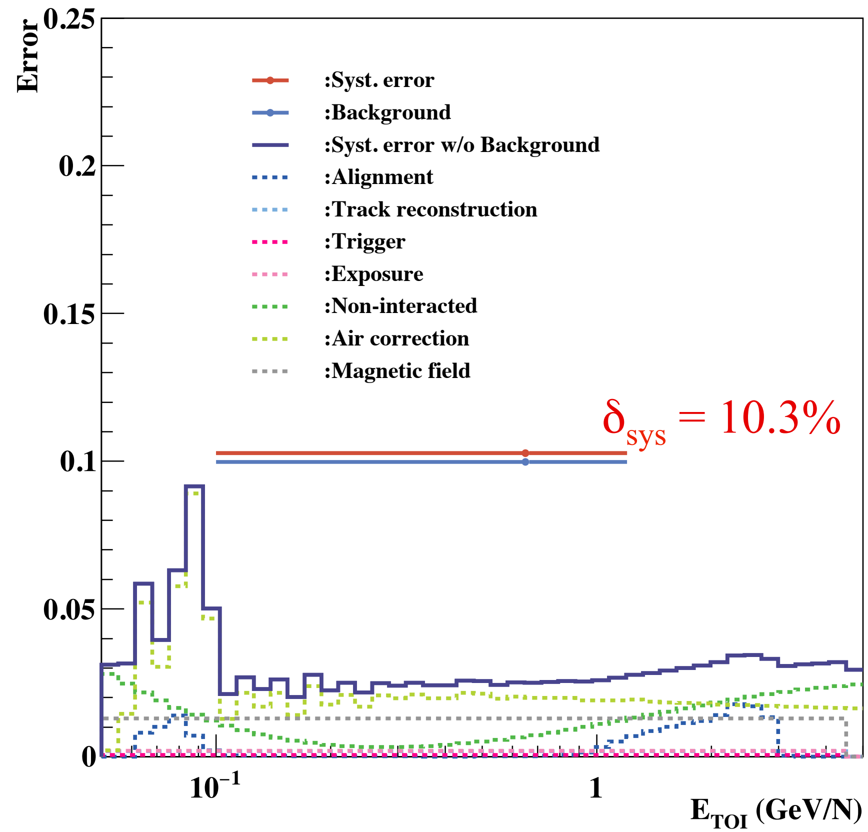

23 Upperlimit of Antideuteron flux

$$\Phi_{\bar{d}}\, dE = \frac{N_{obs}}{S\Omega \cdot T_{live}} \frac{1}{\varepsilon_{single} \cdot \varepsilon_{Q-ID}} \frac{1}{\eta} \frac{1}{(1-\delta_{sys})}$$

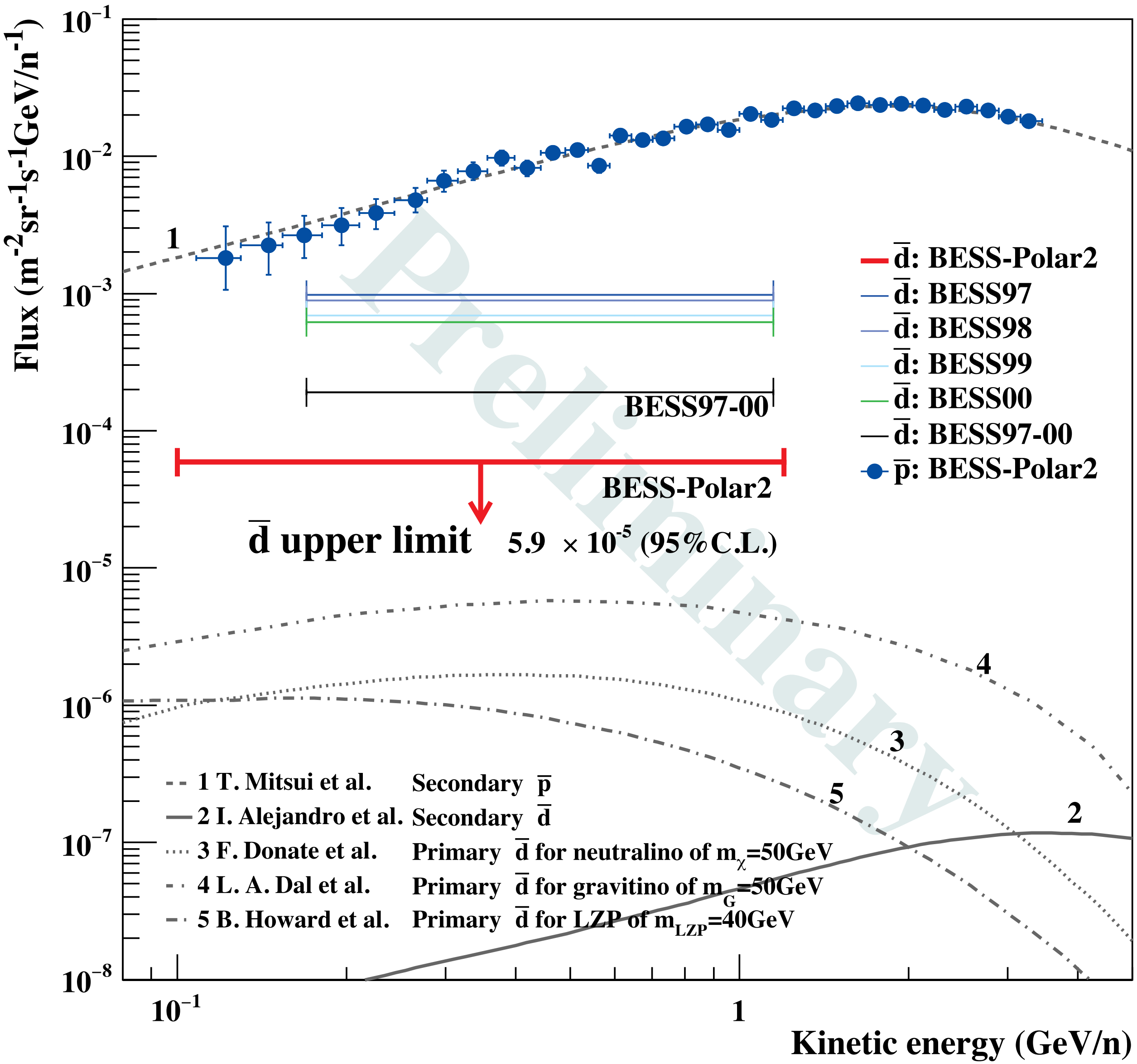

Upper limit on antideuteron flux measured by BESS-Polar II together with earlier published BESS97-00 antideuteron upper limit

$J(\bar{d}) < 5.9 \times 10^{-5}$ $(m^2 sr\ sec\ GeV/n)^{-1}$ (95%C.L.)

- Compared with the data taken in the solar minimum (BESS97), order of magnitude improvement has been achieved.

24 Summary

Antideuteron search

- No antideuteron candidate in BESS-Polar II.

- New upper limit $J(d) < 5.9 \times 10^{-5}\ (m^2 sr\ sec\ GeV/n)^{-1}$ (95%C.L.)
  - 3.1 was taken as the number of the observed antideuteron events for the calculation of 95% C.L. upper limit.
  - In order to obtain the most conservative limit, the effective exposure factors was reduced by using with the systematic error (dsys = 10.3%).

- Compared with the data taken in the solar minimum (BESS97), order of magnitude improvement has been achieved.